



EFFECTS OF JOULE HEATING ON MHD NATURAL CONVECTION IN NON-ISOTHERMALLY HEATED ENCLOSURE

Hakan F. ÖZTOP* and Khaled AL-SALEM**

*Department of Mechanical Engineering, Technology Faculty,
Fırat University, Elazığ, Turkey, hfoztop1@gmail.com

**Department of Mechanical Engineering, King Saud University
Riyadh, Saudi Arabia, kalsalem@ksu.edu.sa

(Geliş Tarihi: 22. 09. 2010, Kabul Tarihi: 16. 12. 2010)

Abstract: In this numerical work, effects of joule heating on natural convection in non-linearly heated square enclosure from right vertical wall were investigated for different Rayleigh numbers and Hartmann numbers. The cavity was considered with adiabatic horizontal walls and cooled left wall. Finite volume method was used to solve governing equations. The calculations have been performed for different Rayleigh numbers ($Ra = 10^4, 5 \times 10^4$ and 10^5), Joule parameter ($J = 0.0, 3.0$ and 5.0) and Hartmann number ($Ha = 0, 10, 20$ and 50). Obtained results are illustrated with streamlines, isotherms, temperature and velocity profiles and mean Nusselt number. It is found that the flow become weaker near the right corner of the cavity due to non-isothermal boundary condition. Both Hartmann number and Joule parameter have important effect on heat transfer and fluid flow.

Keywords: Non-isothermal heater, Natural convection, Joule effect, MHD.

DEĞİŞKEN SICAKLIK ETKİSİNDE BULUNAN BİR OYUKTA MHD DOĞAL TAŞINIMINA JOULE ISITMASININ ETKİSİ

Özet: Bu sayısal çalışmada, farklı Rayleigh ve Hartmann sayıları için sağ cidarı değişken sıcaklığa sahip kare oyukta doğal taşınım ısı transferine joule etkisi incelendi. Oyuğun yatay cidarları yalıtımlı olarak düşünüldü sol taraf ise daha soğuk kabul edilmiştir. Denklemlerin çözümü için sonlu hacim metodu kullanıldı. Hesaplamalar, farklı Rayleigh sayıları ($Ra = 10^4, 5 \times 10^4$ ve 10^5), joule parametresi ($J = 0.0, 3.0$ ve 5.0) ve Hartmann sayısı ($Ha = 0, 10, 20$ ve 50) için yapıldı. Elde edilen sonuçlar, akım çizgileri, eş sıcaklık eğrileri sıcaklık ve hız profilleri ve ortalama Nusselt sayıları ile verildi. Akış yoğunluğu doğrusal olmayan doğrusal olmayan sınır şartından dolayı oyuğun sağ köşesinde daha düşüktür. Hem Hartmann sayısı hem de Joule parametresi ısı transferi ve akış üzerinde etkilidir.

Anahtar Kelimeler: Değişken ısıtıcı, Doğal taşınım, Joule etkisi, MHD.

Nomenclature

B	magnetic field
Cp	specific heat capacity, kJ/kgK
g	acceleration due to gravity, m/s ²
H	height of enclosure, m
Ha	hartmann number, $Ha = LB\sqrt{\sigma/\mu}$
J	joule Parameter, $J = \sigma B^2 Lu / \rho C_p \Delta T$
k	heat conduction coefficient, W/mK
L	length of enclosure, m
\overline{Nu}	average Nusselt number, (Defined in Eq. 7)
Q	rate of internal heat generation per unit volume, W/m ³
p	pressure, N/m ²
Pr	Prandtl number, $Pr = \nu/\alpha$
Ra	Rayleigh number, $Ra = g\beta\Delta TH^3/\alpha\nu$
T	temperature, °C
Tc	temperature at the cold wall, °C
Th	temperature at the hot wall, °C

u, v	velocity, m/s
U, V	dimensionless velocities
x, y	coordinates (-)
X, Y	dimensionless coordinates

Greek Letters

α	thermal diffusivity, m ² /s
σ	fluid electrical conductivity, 1/Ωm
ρ	density, kg/m ³
β	coefficient of thermal expansion of fluid, 1/K
θ	dimensionless temperature, $\theta = (T - T_\infty) / \Delta T$
ν	kinematic viscosity, m ² /s
ϕ	general variable, (-)

Superscript

'	dimensional parameter
---	-----------------------

INTRODUCTION

Heat transfer due to buoyancy forces is an important problem in engineering applications such as floor heating, double pane windows, furnaces and building

applications. These applications are reviewed in earlier literature (De Vahl Davis, 1983, Ostrach, 1972, Catton, 1978). Non-isothermal boundary conditions can be encountered in electrical arc furnaces and rotary burners as given by Gogus et al. (2002). Another application of non-isothermal boundary condition is occurred in case of cylindrical heater, as given by Saeid (2005).

Zahmatkesh (2008) showed the effects of thermal boundary conditions in heat transfer and entropy generation for natural convection. He applied uniform and non-uniform heating and cooling thermal conditions and found that these conditions are of profound influences on the induced flow as well as heat transfer characteristics. Bilgen and Yedder (2007) studied the natural convection problem in enclosure with heating and cooling by sinusoidal temperature profiles on one side. In their case, the equally divided active sidewall is heated and cooled with sinusoidal temperature profiles. It is found that the penetration approaches to 100% at high Rayleigh numbers when the lower part is heated while the higher part is cooled. Basak et al. (2006) performed natural convection in a porous media filled enclosure with uniformly and non-uniformly heated bottom wall. They indicated that non-uniform heating of the bottom wall provides higher heat transfer rates at the central region of the bottom wall whereas mean Nusselt number is lower for non-uniform heating. As an interesting application for non-isothermal boundary condition effect, a study was performed by Varol et al. (2008). In their work, heatline technique was applied to see the heat transport way and found that it is affected from non-isothermal formulation of boundary condition.

Oztop et al. (2009) studied buoyancy induced flow in magnetohydrodynamic fluid filled enclosure with sinusoidally varying temperature boundary conditions. They found that heat transfer was decreased with increasing Hartmann number and decreasing value of amplitude of sinusoidal thermal function. Rahman et al. (2010) performed a numerical work on the conjugate effect of joule heating and magnato-hydrodynamics mixed convection in an obstructed lid-driven square cavity. They indicated that both Hartmann number and Joule heating parameters have notable effect on heat and fluid flow. Beg et al. (2009) carried out a theoretical study of unsteady magnetohydrodynamic viscous Hartmann–Couette laminar flow and heat transfer in a Darcian porous medium intercalated between parallel plates, under a constant pressure gradient. Viscous dissipation, Joule heating, Hall current and nonslip current effects are included as is lateral mass flux at both plates. An analysis is presented by Alim et al. (2008) to investigate the influences of viscous dissipation and Joule heating in the entire thermo-fluid dynamic field resulting from the coupling of buoyancy forced flow with conduction along one side of a heated flat plate of thickness ‘b’. It is found that the values of skin friction coefficient decrease at different position of x for Prandtl number $Pr = 0.05, 0.7, 1.0$ and 4.24 .

The main aim in this numerical work is to study the effects of joule heating on natural convection heat transfer and fluid flow in a square enclosure with non-isothermal heating. Based on authors’ knowledge and the above literature survey clearly indicate that joule heating effects are not studied in earlier. Considered physical model is presented in Figure 1 with coordinates and boundary conditions. As seen from the figure, considered model is a square cavity. The right vertical wall of the enclosure is heated non-linearly. Horizontal walls are adiabatic and the temperature of left vertical wall is constant and lower than that of heated wall. Gravity acts in vertical way. Prandtl number is fixed at 0.71 for whole study.

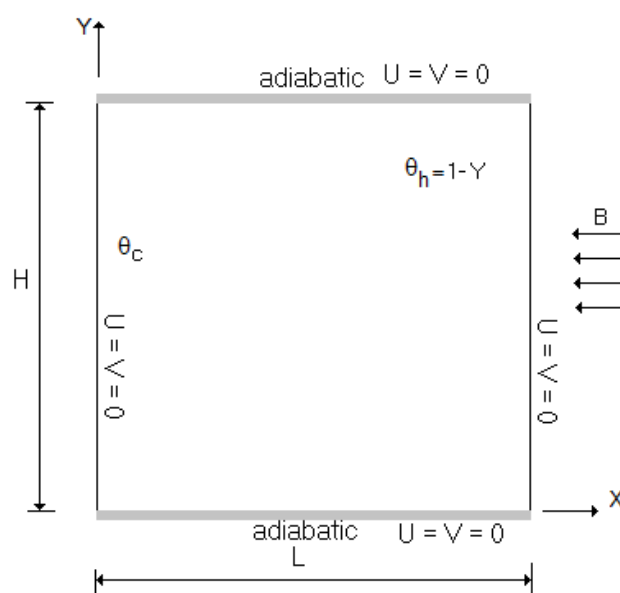


Figure 1. Schematic model with coordinate and boundary conditions.

THEORY

To write governing equations some assumptions are made such as, Fluid is assumed to be Newtonian and incompressible. It is also assumed that flow is laminar and steady and fluid properties are constant and there is no viscous dissipation, Boussinesq approximation are assumed to be valid and radiation heat transfer among sides is negligible. With these assumptions governing equations in dimensional form become,

Continuity equation

$$\frac{\partial u}{\partial x} + \frac{\partial v}{\partial y} = 0 \quad (1)$$

x-Momentum equation

$$u \frac{\partial u}{\partial x} + v \frac{\partial u}{\partial y} = -\frac{1}{\rho} \frac{\partial p}{\partial x} + \nu \left(\frac{\partial^2 u}{\partial x^2} + \frac{\partial^2 u}{\partial y^2} \right) \quad (2)$$

y-Momentum equation

$$u \frac{\partial v}{\partial x} + v \frac{\partial v}{\partial y} = -\frac{1}{\rho} \frac{\partial p}{\partial y} + \nu \left(\frac{\partial^2 v}{\partial x^2} + \frac{\partial^2 v}{\partial y^2} \right) + g\beta(T - T_c) + \nu \nu L^2 B^2 \frac{\sigma}{\mu} \quad (3)$$

Energy equation

$$u \frac{\partial T}{\partial x} + v \frac{\partial T}{\partial y} = \alpha \left(\frac{\partial^2 T}{\partial x^2} + \frac{\partial^2 T}{\partial y^2} \right) + \frac{\sigma B^2 L u}{\rho C_p \Delta T} \nu^2 \quad (4)$$

The above dimensional equations are non-dimensionalized by using following dimensionless parameters as

$$\begin{aligned} (X, Y) &= (x, y) / H \\ \theta &= (T - T_\infty) / \Delta T \\ \Delta T &= T_h - T_\infty \end{aligned} \quad (5)$$

where α is the thermal diffusivity. Dimensionless numbers for the system can be written as follows

$$\begin{aligned} \text{Pr} &= \frac{\nu}{\alpha}, \quad \text{Ra} = \frac{g \beta \Delta T H^3}{\alpha \nu} \\ \text{Ha} &= LB \sqrt{\frac{\sigma}{\mu}}, \quad J = \frac{\sigma B^2 L u}{\rho C_p \Delta T} \end{aligned} \quad (6)$$

The above dimensionless numbers are Prandtl number, Rayleigh number, Hartmann number and Joule parameter, respectively.

Continuity

$$\frac{\partial U}{\partial X} + \frac{\partial V}{\partial Y} = 0 \quad (7)$$

X-momentum

$$U \frac{\partial U}{\partial X} + V \frac{\partial U}{\partial Y} = -\frac{\partial P}{\partial X} + \text{Pr} \left(\frac{\partial^2 U}{\partial X^2} + \frac{\partial^2 U}{\partial Y^2} \right) \quad (8)$$

Y-momentum

$$U \frac{\partial V}{\partial X} + V \frac{\partial V}{\partial Y} = -\frac{\partial P}{\partial Y} + \text{Pr} \left(\frac{\partial^2 V}{\partial X^2} + \frac{\partial^2 V}{\partial Y^2} \right) \quad (9)$$

$$+ \text{Ha}^2 \text{Pr} V + \text{Ra} \text{Pr} T$$

Energy

$$U \frac{\partial \theta}{\partial X} + V \frac{\partial \theta}{\partial Y} = \left(\frac{\partial^2 \theta}{\partial X^2} + \frac{\partial^2 \theta}{\partial Y^2} \right) + J \nu^2 \quad (10)$$

Local Nusselt number and the average Nusselt number is calculated by integrating the local Nusselt number along the wall as given respectively,

$$\text{Nu}_y = -\left(\frac{\partial \theta}{\partial X} \right)_{Y=0}, \quad \overline{\text{Nu}} = \int_0^H \text{Nu}_y dX \quad (11)$$

BOUNDARY CONDITIONS

On the solid walls no-slip boundary conditions were applied. The relevant boundary conditions are given as follows:

On the left wall

$$X = 0, \quad 0 < Y < 1, \quad U = 0, \quad V = 0, \quad \theta = 0 \quad (12.a)$$

On the right wall

$$X = 1, \quad 0 < Y < 1, \quad U = 0, \quad V = 0, \quad \theta = 1 - y \quad (12.b)$$

On the bottom wall

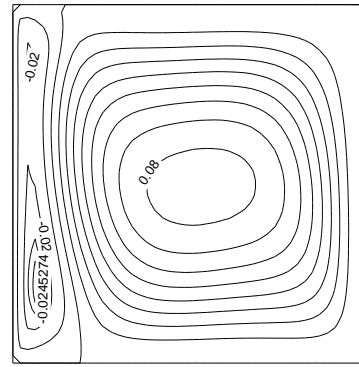
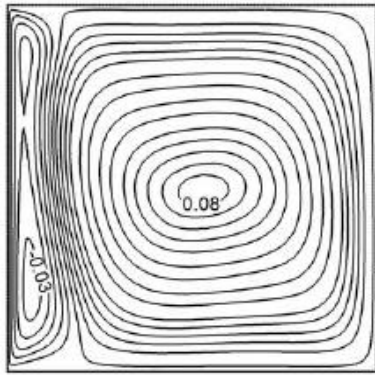
$$Y = 0, \quad 0 < X < 1, \quad U = 0, \quad V = 0, \quad \partial \theta / \partial Y = 0 \quad (12.c)$$

On the top wall

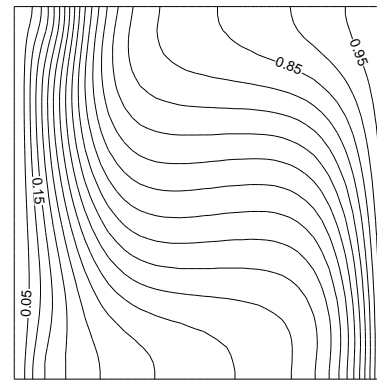
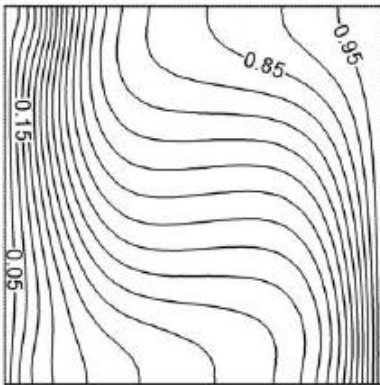
$$Y = 1, \quad 0 < X < 1, \quad U = 0, \quad V = 0, \quad \partial \theta / \partial Y = 0 \quad (12.d)$$

NUMERICAL STUDY AND CODE VALIDATION

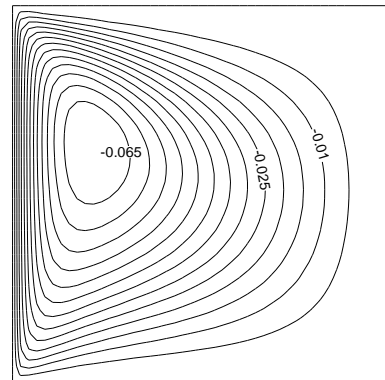
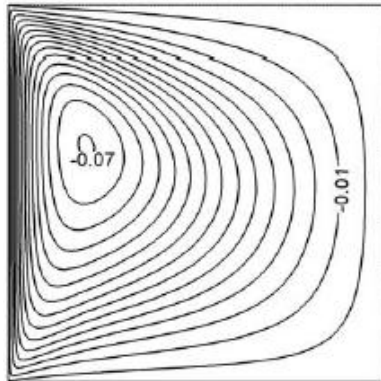
Equations (5-8) are discretized with finite volume method and linearized equations are solved with Tre-Diagonal Matrix Algorithm under boundary conditions as Eq. 12 (a) to (d). SIMPLE solution algorithm of Patankar (1980) was used and SAINTS (software for arbitrary integration of Navier–Stokes equation with turbulence and porous media simulator) code was modified (Nakayama, 1995). A hybrid of the central difference and upwind schemes was used for the convective and diffusive terms. Validation of the code was performed by comparing results with study of Rahman et al. (2010). In their case, Galerkin weighted residual method of finite element formulation is used to solve governing equations. The study is little modified to get similar conditions with Rahman et al. (2010). They are also included Joule effect ($\text{Ha} = 10$ and $J = 0.0$). Results are plotted by streamline and isotherms. The left column belongs to results from literature. Comparison of results shows that they are acceptable. 48×48 grid dimensions are used in this study after making several tests.



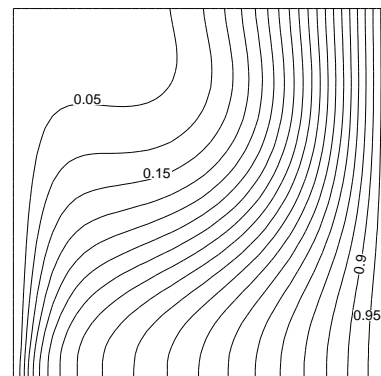
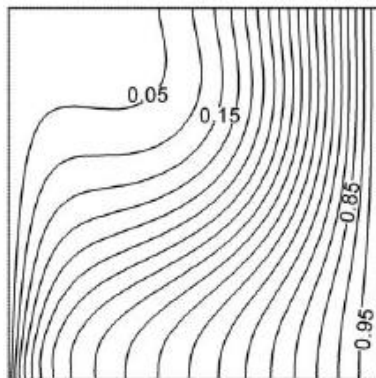
a)



b)



c)



d)

Figure 2. Comparison of results with literature (Rahman vd., 2010) for the case ($Ha = 10$ and $J = 0$) of lid-driven wall and linear heating, streamlines (on the left) and isotherms (on the right).

RESULTS AND DISCUSSION

A numerical study has been performed in this work to see the effects of joule heating and magnetic field on non-isothermally heated square enclosure. Study is performed for different Rayleigh numbers, Hartmann numbers and Joule parameter. It is noticed that the similar values are chosen with literature. Range of Rayleigh number supplies the laminar flow regime. Results will be present by streamlines, isotherms, Nusselt numbers, temperature and velocity profiles.

Figure 3 illustrates the streamlines (on the left) and isotherms (on the right) to show effects of Rayleigh

number for $Ha = 0.0$ and $J = 1.0$. As indicated above that the right vertical wall of enclosure is heated non-linearly. The temperature increases along the wall in the positive y direction. Thus, the cavity is mostly heated with the joule effect. For $Ra = 104$, two circulation cells were formed. The main cell rotates in counter clockwise and other one sits at the right top corner and it turns in clockwise. The heated part is effective on formation of the big main cell (Figure 3 (a)). As shown from the isotherm for the same case, temperature rises from heated part of the non-linearly heated wall through the left top corner. Two areas (hot

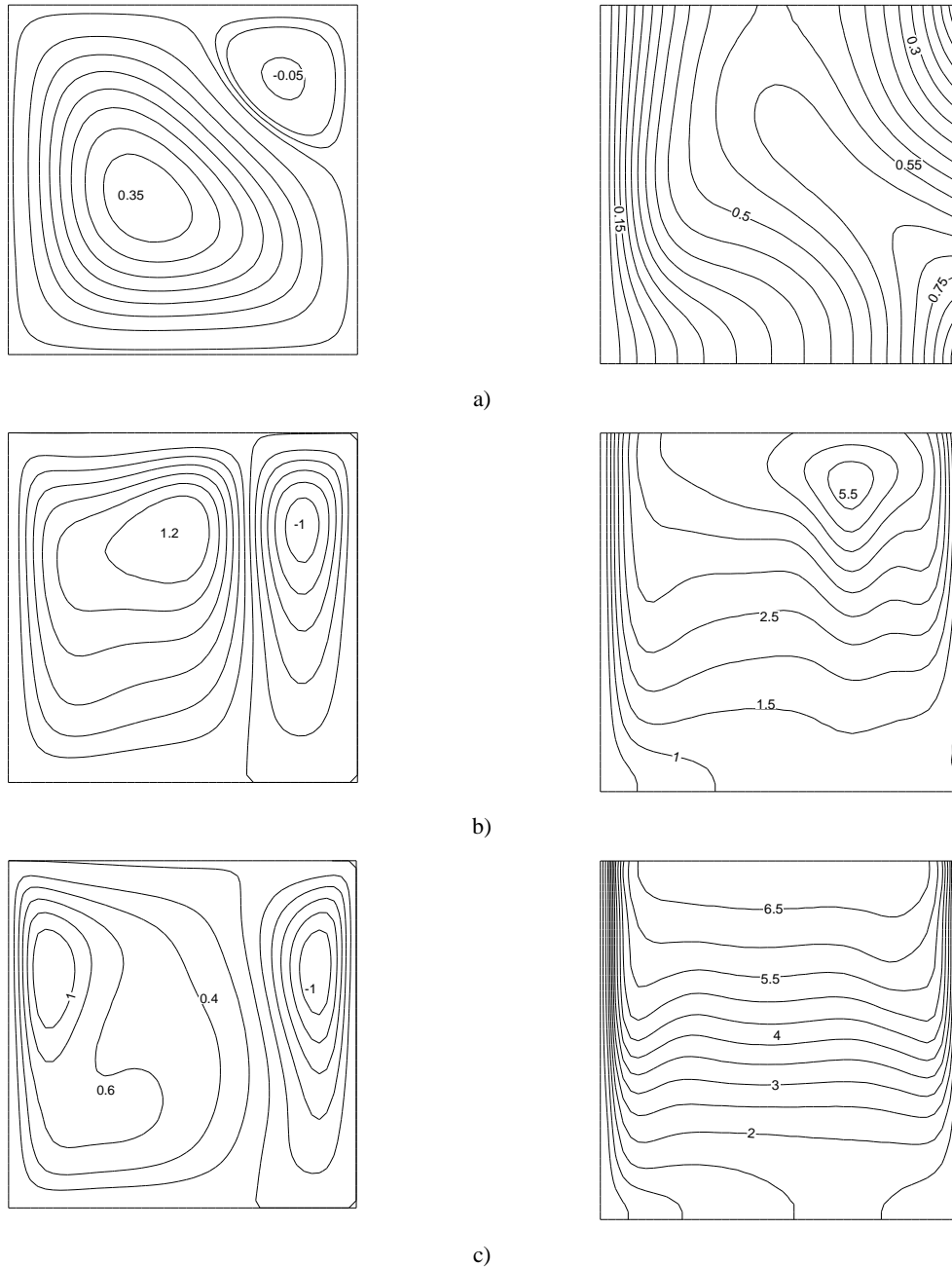


Figure 3. Streamlines (on the left) and isotherms (on the right) for $Ha = 0$ and $J = 1.0$ for different Rayleigh numbers a) $Ra = 10^4$, b) $Ra = 5 \times 10^4$, c) $Ra = 10^5$.

and old) are formed on right wall. With increasing of Rayleigh number, the left cell becomes bigger and it locates along the right vertical wall (Figure 3 (b)). For $Ra = 4 \times 10^5$, minimum value of stream function is obtained as -1. Joule heating becomes more effective even joule parameter is constant. Thus, isotherms try to show parallel variation to the top and bottom walls. This case is clearer for $Ra = 10^5$ (Figure 3 (c)).

Figure 4 (a) to (c) presents temperature and flow field for different Hartmann number for $Ra = 10^5$ and $J = 0.0$. As seen from the figure, two cells (main cell and a small cell at right top corner) are formed inside a cavity for all

values of Hartmann numbers. The maximum values of stream function decreases with increasing of Hartmann number. It means that increasing of magnetic field reduces the flow velocity. Meanwhile, there is no big change on small circulation cell at right top corner. Thermal boundary layer at the right bottom corner becomes larger with increasing of Hartmann number. Plume-like temperature distribution is shown on 75% of heated wall. Figure 5 (a) to (c) indicates that effects of joule heating. As indicated above that four values of joule parameters are studied as $J = 0.0, 1.0, 3.0$ and 5.0 . The joule parameter is the most important

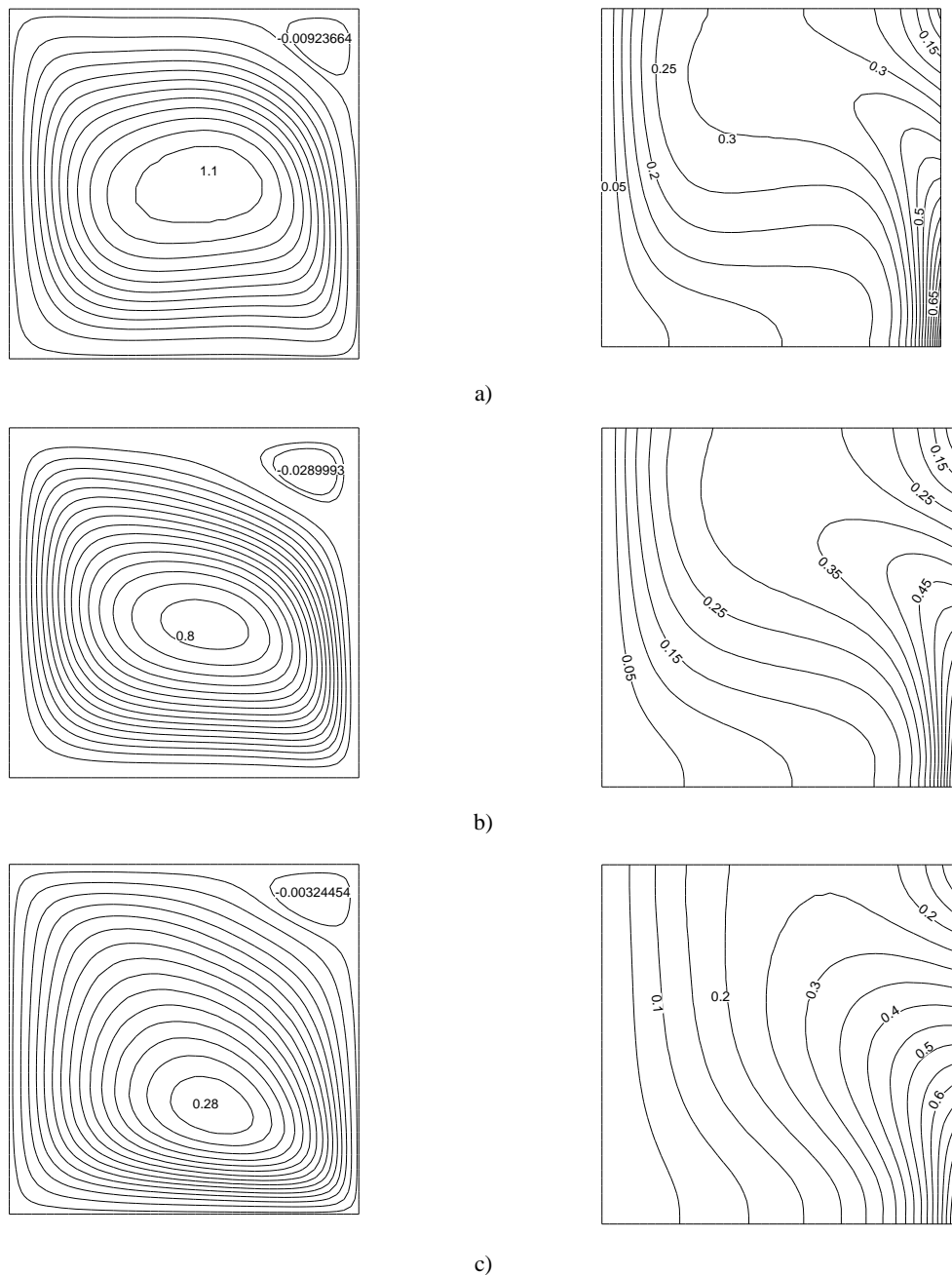


Figure 4. Streamlines (on the left) and isotherms (on the right) for $Ra = 10^5$ and $J = 0.0$ for different Hartmann numbers, a) $Ha = 10$, b) $Ha = 20$, c) $Ha = 5$.

parameter for this study. When $J = 1$ (Fig 5 (a)), flow and thermal field are similar to earlier case. But increasing of joule parameter enhances the flow strength. It is an interesting result that minimum and maximum values of stream function are the same for $J = 3.0$ and 5.0 in Figure 5 (b) and (c), respectively. Internal heating or joule heating becomes dominant for $J = 5.0$ and isotherms are almost parallel to top and bottom side. It means that Joule parameter can be a control element for heat and fluid flow.

These figures are plotted to see the effects of Joule parameters on variation of velocity and temperature. As seen from Figure 6 (a), temperatures at the middle of the enclosures are identical for $J = 0$ and 1. But they are increased with increasing of Joule parameter. Similarly, velocities are strongly affected from the Joule parameter as given in Figure 6 (b). There are negative and positive values on velocities from $J = 0$ to $J = 3$ at the middle of the cavity. However, the main cell, which rotates in counterclockwise (in Figure 5), becomes dominant.

Figure 6 (a) and (b) illustrates the temperature and velocity profiles at $Ra = 104$ and $Ha = 10$, respectively.

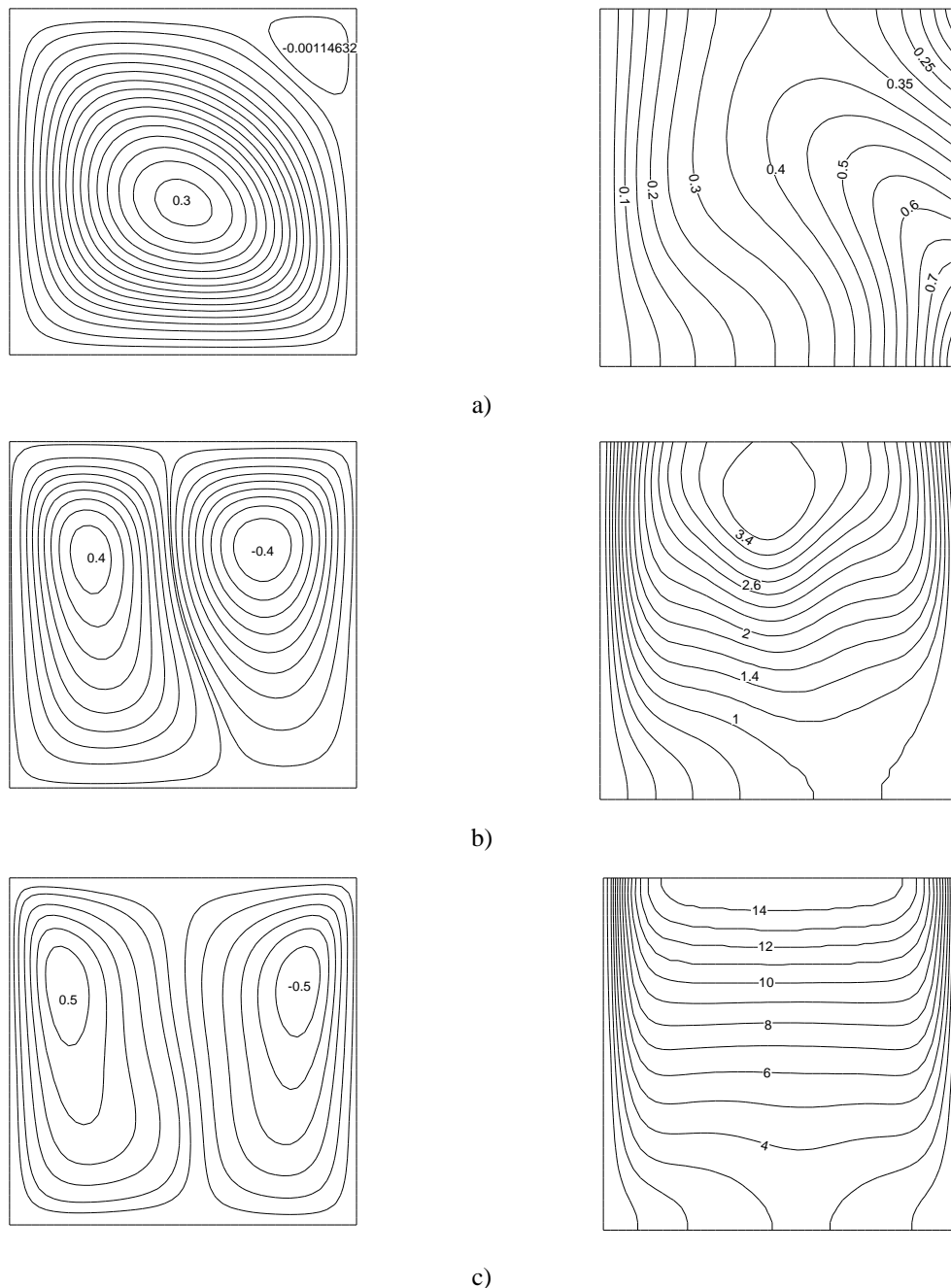


Figure 5. Streamlines (on the left) and isotherms (on the right) for $Ra = 10^4$ and $Ha = 10.0$ for different Joule parameter, a) $J = 1.0$, b) $J = 3.0$, c) $J = 5.0$.

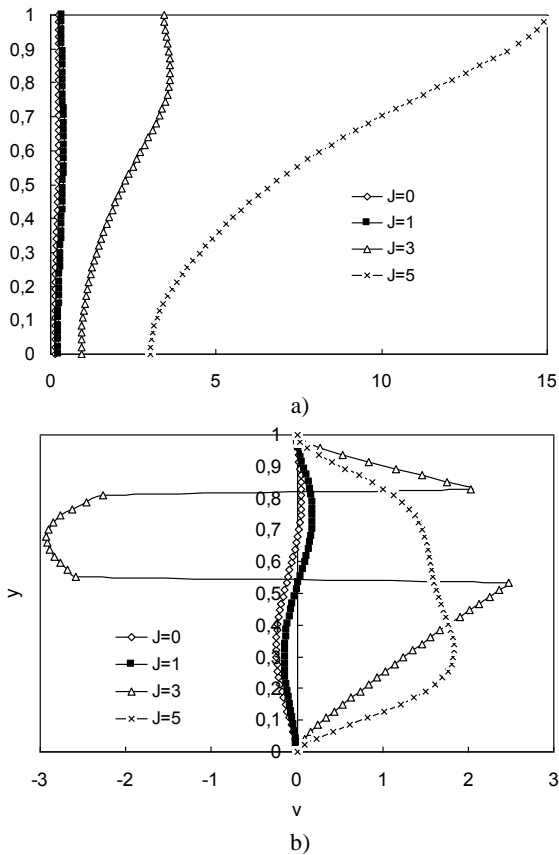


Figure 6. a) Temperature, b) Velocity profiles at the middle of the enclosure for different Joule parameter for $Ra = 10^4$ and $Ha = 10$.

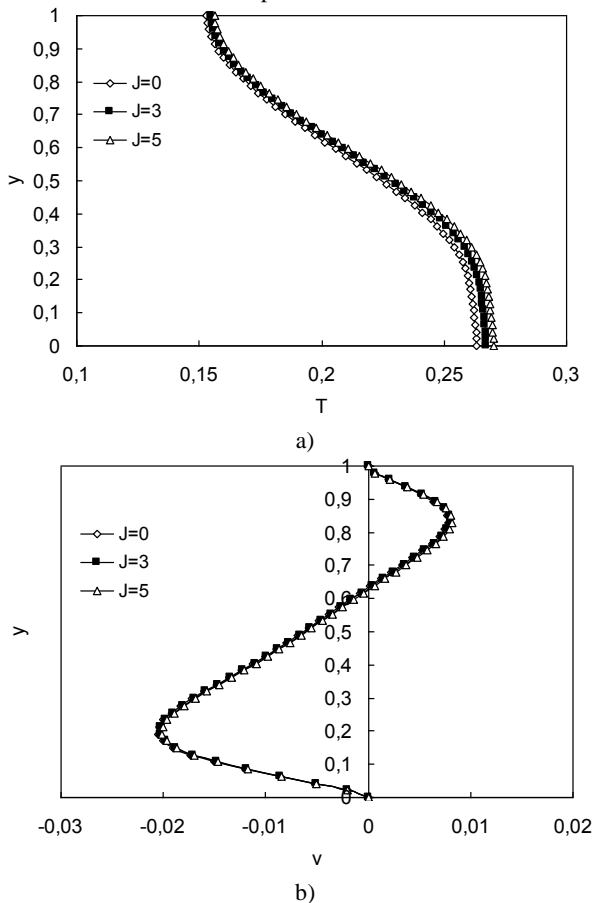


Figure 7. a) Temperature, b) Velocity profiles at the middle of the enclosure for different Joule parameter for $Ra = 10^4$ and $Ha = 50$.

With increasing of Hartmann number, Joule number becomes insignificant on both velocity and temperature distribution as given in Figure 7 (a) and (b). The temperatures become high at the top and lower at the bottom even the enclosure is heated from the bottom wall of the right vertical wall. Velocity profiles show that rotating fluid in clockwise become dominant and maximum velocity value is -0.02 . It means that increasing of Hartmann number decreases the fluid velocity.

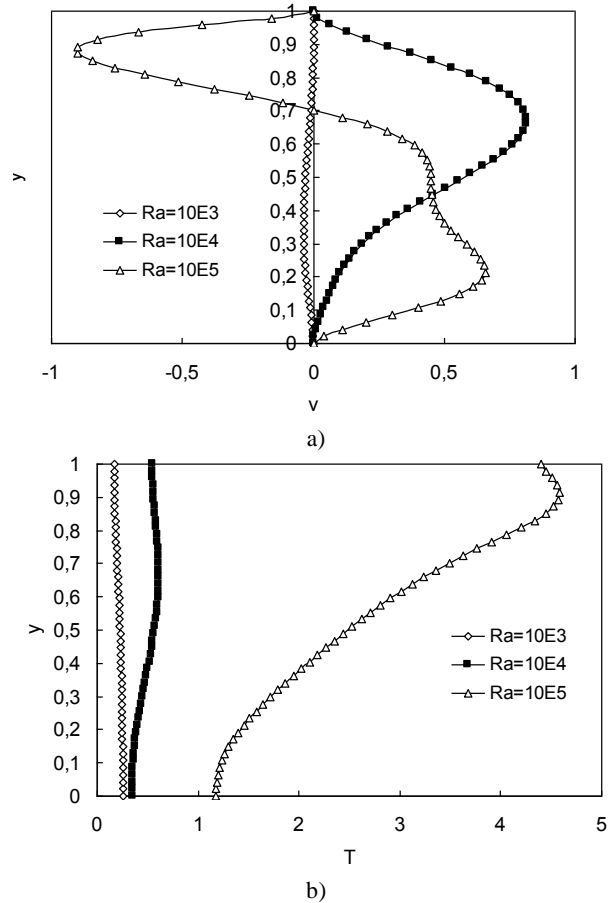


Figure 8. a) Temperature, b) Velocity profiles at the middle of the enclosure for different Rayleigh number $J = 0$ and $Ha = 0$.

Figure 8 is plotted to see the effects of Rayleigh number on temperature and velocities for constant Hartmann number and Joule parameter. Figure 8 (a) illustrates the velocity profiles. For $Ra = 103$, velocity profile is almost due to domination of conduction mode of heat transfer. With increasing of Rayleigh number to $Ra = 104$, a parabolic shaped velocity profiles were formed due to increasing of domination of convection heat transfer. Due to forming of double circulation cell, both negative and positive profiles occur inside the cavity. Velocity value is very high near the ceiling of the cavity. Similarly, temperature distribution indicates that conduction heat transfer is dominant for $Ra = 103$ as seen Figure 8 (b). Temperature values at the middle of the enclosure increases with increasing of Rayleigh number.

Mean Nusselt numbers are listed in Table 1 for all studied parameters. The table shows that Hartmann number decreases the heat transfer as given in literature (Rahman vd., 2010). For higher values of Hartmann number, heat transfer becomes almost constant. Negative value of mean Nu indicates the domination of joule heating inside the cavity. But heat transfer increases with increasing of Joule parameter. Ra number also increases the heat transfer which is directly related with temperature difference for a square enclosure.

Table 1. Variation of mean Nusselt numbers for different parameters.

Ra	Ha	J	Nu
104	10	0	1.33
104	0	0	1.39
104	10	1	0.81
104	10	3	-4.93
104	10	5	-46.36
104	20	0	1.29
104	50	0	1.29
104	10	1	1.28
104	50	3	1.27
104	50	5	1.27
105	10	0	1.61
105	10	3	-196
105	10	5	-290

CONCLUSIONS

In this study, temperature and flow field are investigated for a cavity with heated non-isothermally from one vertical wall. Effects of joule heating are investigated with magneto-hydrodynamic fluid. Thus, these Hartmann number and Joule parameters are included into governing equations. Graphical results for studied parameters were presented comparatively and discussed in detail in earlier sections. The main findings can be listed as below

- Both magnetic field and Joule parameter have strong effect on heat and fluid flow.
- Non-uniform boundary condition has strong effect near the heated vertical wall.
- Double cells were formed for all values of Rayleigh number at $J \geq 1$. Increasing of Rayleigh number enhances the values of stream function.
- Positive stream functions are decreased with increasing of Hartmann number and thermal boundary layer becomes larger.
- For the highest value of Hartmann number, Joule parameter becomes insignificant.

ACKNOWLEDGEMENT

The authors wish to express their very sincerely thanks to the reviewers for the valuable comments and suggestions.

REFERENCES

- Abo-Eldahab, E.M., El Aziz, M. A., Viscous dissipation and Joule heating effects on MHD-free convection from a vertical plate with power-law variation in surface temperature in the presence of Hall and ion-slip currents, *Applied Mathematical Modelling*, 29, 579–595, 2005.
- Alim, M.A., Alam, Md. M., Mamun, A.A., Hossain, B, Combined effect of viscous dissipation and joule heating on the coupling of conduction and free convection along, *International Communications in Heat and Mass Transfer*, 35, 338–346, 2008.
- Basak, T., Roy, S., Paul, T., Pop, I., Natural convection in a square cavity filled with a porous medium: effects of various thermal boundary conditions, *Int. J Heat Mass Transfer*, 49, 1430–1441, 2006.
- Bég, O.A., Zueco, J., Takhar, H.S., Unsteady magneto-hydrodynamic Hartmann–Couette flow and heat transfer in a Darcian channel with Hall current, ionslip, viscous and Joule heating effects: Network numerical solutions, *Commun. Nonlinear Sci Numer Simulat*, 14, 1082–1097, 2009.
- Bilgen, E., Yedder, R.B., Natural convection in enclosure with heating and cooling by sinusoidal temperature profiles on one side, *Int. Comm. Heat Mass Transfer*, 50, 139–150, 2007.
- Catton, I., Natural convection in enclosures. In: *Proceedings of the sixth heat transfer conference*, Toronto, Canada; 1978.
- De Vahl Davis, G., Natural convection of air in a square cavity: a benchmark solution, *Int. J. Numer. Meth. Fluids* 3, 249–264, 1983.
- Gogus, Y.A., Camdali, U., Kavsaoglu, M., Exergy balance of a general system with variation of environmental conditions and some applications, *Energy*, 27, 625–646, 2002.
- Nakayama, A., *PC-aided numerical heat transfer and convective flow*, CRC Press, 1995.
- Ostrach, S., Natural convection in enclosure. In: Harnett JP, Irvine TF, editors. *Advances in heat transfer*, NY: Academic Press; 8, 161–227, 1972.

Oztop, H.F., Oztop, M., Varol, Y., Numerical simulation of magnetohydrodynamic buoyancy-induced flow in a non-isothermally heated square enclosure, *Comm. in Nonlinear Sci. Numerical Simulation*, 14, 770-778, 2009.

Patankar, S.V., Numerical Heat Transfer and Fluid Flow, *Hemisphere, McGraw-Hill*, Washington DC, 1980.

Rahman, M.M., Alim, M.A., Sarker, M.A., Numerical study on the conjugate effect of joule heating and magneto-hydrodynamics mixed convection in an obstructed lid-driven square cavity, *Int. Comm. Heat Mass Transfer*, 37, 524-534, 2010.

Saeid, N.H., Natural convection in porous cavity with sinusoidal bottom wall temperature variation. *Int Commun Heat Mass Transfer*, 32, 454 – 463, 2005.

Varol, Y., Oztop, H.F., Mobedi, M., Pop, I., Visualization of natural convection heat transport using heatline method in porous non-isothermally heated triangular cavity, *International Journal of Heat and Mass Transfer*, 51, 5040-5051, 2008.

Zahmatkesh, I., On the importance of thermal boundary conditions in heat transfer and entropy generation for natural convection inside a porous enclosure, *Int. J. Thermal Sciences*, 47, 339-346, 2008.